Available online at www.sciencedirect.com

ScienceDirect

Procedia Engineering 97 (2014) 1618 – 1625

Procedia Engineering

www.elsevier.com/locate/procedia

Influence of moisture in the Gypsum moulds made by 3D Printing

S. S. Bobby[1]*, and Sarat Singamneni [2]

[1,2]*School of Engineering, AUT University, Auckland 1010, New Zealand*

Abstract

The process of rehydration of calcium sulphate hemihydrate (CaSO4. $0.5H_2O$) to the crystallization of gypsum which is chemically known as calcium sulphate dihydrate (CaSO4. $2H_2O$) is based on the amount of water added back. Plaster moulds are used to produce both ferrous and non-ferrous castings through investment casting process using slip casting techniques conventionally. The percentage water influences the properties of moulds and castings. Taking advantage of the rapid casting process a study was conducted to measure the effect of moisture in the moulds produced by three dimensional printing and it was found that the percentage moisture is directly proportional to the green compressive strength. L9 orthogonal array and the Box-Behnken design of experiments were used to study the effect of the percentage moisture in the mould.

© 2014 Published by Elsevier Ltd. This is an open access article under the CC BY-NC-ND license (http://creativecommons.org/licenses/by-nc-nd/3.0/).
Selection and peer-review under responsibility of the Organizing Committee of GCMM 2014

Keywords: Hymihydrate, Dihydrate, 3D Printing, L9 Orthogonal Array, Box-Behnken DOE, Green Compressive Strength

1. Introduction

Hydration of hemihydrate determines the properties of gypsum and it is influenced strongly by water and the properties of hemihydrate. Calcium sulphate hemihydrate reacts with water relatively rapidly to regenerate calcium sulphate dihydrate. This process turns powdery hemihydrate into the solid mass of dihydrate that we commonly think of as set plaster or Gypsum plaster ($CaSO_4$. $2H_2O$) **[1]**. Set plaster is made up of entangled needles of gypsum crystals obtained by a solution mediated phase transition of calcium hemihydrate ($CaSO_4$. $0.5H_2O$) as the reaction given below.

$$CaSO_4.0.5H_2O+1.5H_2O \rightarrow CaSO_4.2H_20 \quad (1)$$

The cohesion and the mechanical strength of the solid are due to both entanglement and inter–crystalline interaction **[2].** There are six types of the reaction mechanisms in general for the gypsum hydration process; Dissolution, Diffusion and Precipitation are the most common among them. Dissolution is the mechanism in which salts break into ions. The amount that will dissolve depends on the dissolution product of the salt, whereas diffusion is a spontaneous process, the water molecule makes a random walk about a central location since by kinetic theory the

* Corresponding author. Tel.: +6499219999

E-mail address: solaman.selvaraj@aut.ac.nz

1877-7058 © 2014 Published by Elsevier Ltd. This is an open access article under the CC BY-NC-ND license (http://creativecommons.org/licenses/by-nc-nd/3.0/).
Selection and peer-review under responsibility of the Organizing Committee of GCMM 2014
doi:10.1016/j.proeng.2014.12.312

mean velocity of a pixel is zero when it is not subjected to any external forces. Due to collisions with neighbouring molecules the motion of the particle is characterized by a mean free path which tends to limit the pixel. But since there is no potential field acting to restore a pixel to its original position, it is free to move through the fluid, in which it is located **[13]** while the precipitation involves many individual steps and kinetic processes **[14].** The plaster powder is categorised into two forms based on the process, α-plaster through wet process and β-through dry process. Many studies have been carried out on both types of plaster including the determination of the mechanisms and factors governing the hydration reaction **[3, 4]**. The gypsum crystals of the α-plaster are well formed with a high degree of entanglement resulting from the gradual evolution of the microstructure. In the β-plaster, the gypsum crystals are shorter and stacked rather than entangled **[8]**. Singh et al. analysed and believed that the morphological differences between α and β crystals are from different hydration mechanisms, causing the α-crystals to be more regular in structure than the β-crystals as shown in **Fig 1**. The pore structure of the α-plaster evolves gradually to form a homogenous structure consisting of interlocking gypsum crystals while the β-plaster evolves more rapidly after an infiltration period to form shorter, fractured needles, giving rise to a less homogeneous structure **[9].** Water is the key element in the hydration process since it works not only as reactant but also as carrying liquid. From equation (1) it can be seen that the amount of water is needed as reactant for the hydration reaction of both types of hemihydrates. However, an excess amount of water is necessary for the hydration to take place due to that all hemihydrate particles need to be covered with a water layer to promise enough fluidity during the induction period. The required amount of α and β-hemihydrates are 33wt. % and 61wt. % respectively for the hydration reaction. Water has a bigger influence on the flowability of the gypsum plaster which is probably due to its smaller surface area **[10]**.

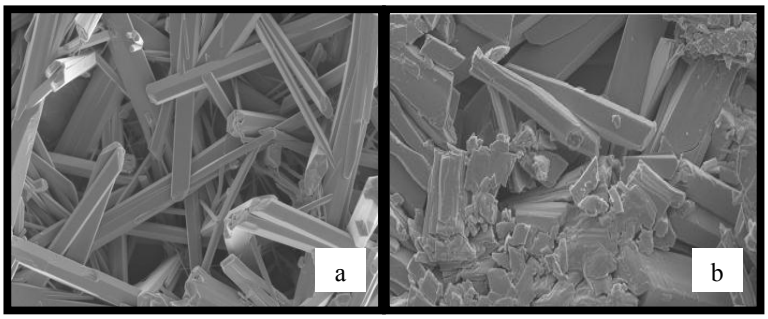

Fig.1: SEM images of (a) α-plaster and (b) β-plaster [9]

The void fraction is strongly influenced by the addition of water which develops two types; the first type is caused by the volume contraction during hydration because of the conversion of hemihydrate to dihydrate via solution phase. This volume shrinkage increases linearly with the hydration degree which is influenced by water and the hemihydrate property. The second type is caused by the evacuation of excess water after hydration. The influence of the water content on the strength of the gypsum moulds was investigated by Yu et al and found that when the amount of water increases the void fraction increases and leading to a weaker bond between the gypsum crystals, resulting decreased strength **[10]**. Higher water ratio in the gypsum mould material leads to bigger void fraction and resulting lower compressive strength **[11]**. Bonds between the faces of the crystals are weakened by water adsorption **[5, 6]** at grain boundaries allows crystals to slip against each other under stress **[7].** Addition of additives could prevent the water adsorption at grain boundaries of gypsum. The commercial gypsum bonded investment have the compressive strength of 0.1-0.6MPa and it depends on the type of silica sand is used **[12].** All these findings are with respect to slip casting process but there is a lack of data available explaining the hydration of the gypsum when used in three dimensional printing.

In 3DP an ink-jet nozzle system delivers fluid on the powder bed selectively in a two-dimensional pattern using drop-on-demand by print head driven by customized software which receives data from a CAD system. When the fluid initially comes into contact with the powder mixture, it immediately flows outward (on the microscopic scale)

from the point of impact by capillary action, dissolving the adhesive within the first few seconds. A droplet of fluid, typically having a volume of about 100pl, may spread to a surface area of about 100µm once it comes into contact with the powder mixture. As the solvent dissolves the adhesive material system and at least one of the filler and binder materials, the fluid viscosity increases dramatically, arresting further migration of the fluid from the initial point of impact. Within a few minutes, the fluid with dissolved binder material infiltrates the less soluble and slightly porous particles, forming bonds between the filler particles **[15]**. The aim of this research is to understand the role of water in the gypsum material system used for 3D printing and ascertain the the effects on specific properties.

2. Selection of the materials

The important properties of any moulding sand are refractoriness, permeability, cohesiveness, green strength, dry or baked strength, flowability or plasticity, adhesiveness, and collapsibility while the coefficient of thermal expansion should be low **[16]**. There are various types of refractory sands used in sand casting namely Silica sand, Zircon sand, Olivine sand and etc. Out of which Silica sand is widely used because of it is cheap and easily available, chemically immune to molten metal and the lack of decay **[17]**. In this research New Zealand's high purity, near white and round shaped silica sand with AFS 60-65 was used and the β-hemihydrate plaster is used as the binder. A preliminary study were conducted with varying percentage compositions of silica sand (50%-90%), β-hemihydrate (10%-75%) and water (1% - 15%) to select the most appropriate combinations of factor levels. Rectangular test specimens were printed and checked for dimensional accuracy, thump pressure strengths. Based on the results three levels of the each material system were selected **[16]**.

3. Experiments, Results, and Discussion

Based on the results obtained thorough the preliminary experiments the levels shown in Table 1 are selected for each ingredient. Taguchi L9 Orthogonal Array was used to find the influencing factors considering the responses; Green Volume Error, Green Density, Green Compressive Strength and post backing residual moisture content. Each experiment was conducted twice as per the L9 orthogonal experimental design. ASTM standard Compressive strength test specimens (ϕ50mm x h50mm) were printed and the dimensional difference and the compressive strength were measured and recorded as given in Table-2.

Table-1: Process parameters and their levels

Parameters	Low level	Middle level	High level
Silica Sand	67%	57%	47%
β- Hemihydrate	33%	43%	53%
Water	2%	3%	4%

Level	Green Volume Error, %			Green Density, g/cm3			Green Compressive Strength, KPa		
	Silica Sand	β-HH	Water	Silica Sand	β-HH	Water	Silica Sand	β-HH	Water
1	36.04	20.48	18.27	36.02	33.71	38.47	13.5	12.05	13.31
2	16.60	20.33	15.30	44.13	44.09	41.98	21.42	17.00	17.79

3	15.05	26.89	34.13	36.39	38.74	36.09	13.22	19.08	17.03
Δ	20.99	6.56	18.83	8.11	10.38	5.89	8.2	7.03	4.48
Rank	3	1	2	2	1	3	1	2	3

The Table-2: calculated rank for various responses based on signal to noise ratio

Three forms of signal to noise (S/N) ratios were considered; smaller the better, larger the better, and nominal the better to rank each response. Green volume error was ranked as per smaller the better, Green Density and Green Compressive strength were ranked as per larger the better (Table-2). Based on the rank shown in Table 3, the percentage of hemihydrate has the largest effect and the percent silica sand has the lowest effect on the green volume error, the hemihydrate and water percentages have the largest and the lowest effects respectively on the green bulk density. Silica Sand percentage has the largest effect and the percentage of moisture has the lowest effect on the green compressive strength. To find the optimum composition of the mixture the Box-Behnken design of experiment was used and ANOVA was conducted to find the influencing parameters for each response. The following are the second order quadratic models developed for critical responses:

$$Y\ (\%\ \text{Green Volume Error}) = 12.3314 - 0.2174X_1 + 9.8269X_2 - 0.0087X_1^2 - 3.0018X_2^2 + 0.1637X_1X_2 \quad (1)$$

$$Y\ (\text{Green Bulk Density}) = 1.5361 - 0.0032X_1 - 0.0361X_2 - 0.0002X_1^2 - 0.0086X_2^2 + 0.0018X_1X_2 \quad (2)$$

$$Y\ (\text{Green Compressive Strength}) = 3261.2776 - 120.5620X_1 - 229.6565X_2 + 0.9928X_1^2 - 34.9151X_2^2 + 9.3668X_1X_2 \quad (3)$$

$$Y\ (\text{Moisture Content}) = -5.0475 + 0.6385X_1 - 0.0450X_2 - 0.0188X_3 - 0.2567X_4 - 0.0082X_1^2 - 0.0443X_2^2 + 0.0000X_3^2 - 0.0787X_4^2 + 0.0097X_1X_2 + 0.0002X_1X_3 + 0.0136X_1X_4 - 0.0015X_2X_3 + 0.1288X_2X_4 + 0.0003X_3X_4 \quad (4)$$

Equations (1) – (4) were used to calculate model predicted values for each response, equation (1,2 &3) were written by considering the two variables of percentage hemihydrate and percentage water whereas equation (4) was written by considering additionally two more other variables; baked temperature and baked time. The graphs were drawn for both experimental and model predicted values of Green Volume Error (Fig. 2), Green Bulk Density (Fig.3), Green Compressive Strength (Fig.4), and Moisture content (Fig.5) including percentage deviation of the same.

As seen from Fig 2, the percentage green volume error is higher when the hemihydrate percentage is lower (33%) with 2% of water on the other hand the percentage silica sand is higher (67%) which gives more pore space to grow the gypsum crystals during the hydration process leads to specimen swelling which is the reason for the dimensional change in excess. Whereas when the percentage hemihydrate is higher (53%) with the same 2% water the volume change is lesser or nil as lower silica sand restricts the growth of the gypsum crystals. The hemihydrate being more in quantity, more nuclei begin, thus restricting growth of individual crystals and controlling dimension during the rehydration process. **Fig. 3** shows the experimentally measured and model predicted bulk density which is associated with the strength of the mould and the quality of the casting. In general density is directly proportional to porosity, i.e. when the porosity or permeability decreases density increases and vice versa. However, less porous structure will affect the shake out of the mould after solidification. Obtaining the optimum density and the porosity / permeability is a challenging job in mould preparation. The amount of addition of water, particle size and shape, gypsum crystal shape and size, interlocking structure of the gypsum crystals and the bonding structure are the other parameters defined by the mould density. There was no much difference in values observed between experimentally measured density and the model predicted density. When the percentage of water increases it increases the void fraction and will increase the porosity / permeability.

Table-3: Experimental and Model Values of the various responses

Run	Natural Values		Green Volume Error, %		Error	Green Bulk Density, g/cm^3		Error	Green Compressive Strength, KPa		Error
	% β-HH	% Water	Exp.	Model		Exp.	Model		Exp.	Model	
1	33	2	16.29	14.09	2.2	1.22	1.27	-0.05	276.88	383.03	-27.71
2	33	2	14.59	14.09	0.5	1.29	1.27	0.02	436.13	383.03	13.86
3	33	2	11.1	14.09	-2.99	1.3	1.27	0.03	312.54	383.03	-18.40
4	33	3	13.79	14.31	-0.52	1.21	1.25	-0.04	403.53	287.86	40.18
5	33	3	15.08	14.31	0.77	1.22	1.25	-0.03	429.68	287.86	49.27
6	33	4	9.01	8.53	0.48	1.25	1.21	0.04	93.71	122.86	-23.73
7	33	4	9.01	8.53	0.48	1.22	1.21	0.01	65.36	122.86	-46.80
8	33	4	7.59	8.53	-0.94	1.23	1.21	0.02	75.55	122.86	-38.51
9	43	2	6.87	8.54	-1.67	1.16	1.15	0.01	142.6	119.25	19.58
10	43	2	8.31	8.54	-0.23	1.15	1.15	0	205.42	119.25	72.25
11	43	2	9.55	8.54	1.01	1.18	1.15	0.03	95.41	119.25	-19.99
12	43	3	9.37	10.4	-1.03	1.14	1.15	-0.01	72.49	117.76	-38.44
13	43	3	11.1	10.4	0.7	1.15	1.15	0	99.65	117.76	-15.38
14	43	3	9.72	10.4	-0.68	1.14	1.15	-0.01	37.35	117.76	-68.28
15	43	3	12.12	10.4	1.72	1.17	1.15	0.02	95.41	117.76	-18.98
16	43	3	12.12	10.4	1.72	1.16	1.15	0.01	91.67	117.76	-22.15
17	43	4	6.13	6.26	-0.13	1.11	1.13	-0.02	80.78	46.43	73.99
18	43	4	4.63	6.26	-1.63	1.11	1.13	-0.02	86.45	46.43	86.20
19	43	4	6.49	6.26	0.23	1.11	1.13	-0.02	78.6	46.43	69.29
20	53	2	1.58	1.25	0.33	1	1	0	69.77	54.04	29.11
21	53	2	1.77	1.25	0.52	0.95	1	-0.05	58.91	54.04	9.01
22	53	2	1.58	1.25	0.33	0.99	1	-0.01	71.3	54.04	31.94
23	53	3	3.13	4.75	-1.62	1.04	1.02	0.02	120.7	146.21	-17.45
24	53	3	3.69	4.75	-1.06	1.04	1.02	0.02	106.44	146.21	-27.20
25	53	4	1.39	2.24	-0.85	0.99	1.02	-0.03	169.26	168.55	0.42
26	53	4	3.13	2.24	0.89	1.01	1.02	-0.01	141.08	168.55	-16.30
27	53	4	3.69	2.24	1.45	1.05	1.02	0.03	222.73	168.55	32.14

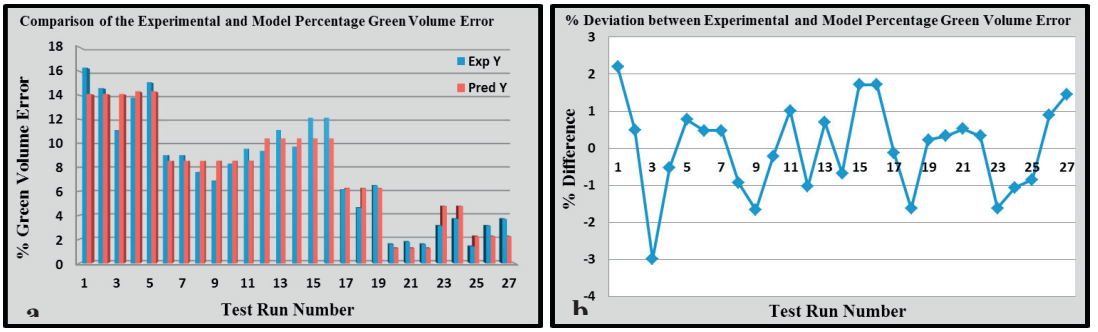

Fig. 2. (a) Comparison of Experimental and Model predicted Green Volume Error, (b) Percentage Deviation of Experimental and Model Predicted Green Volume Error.

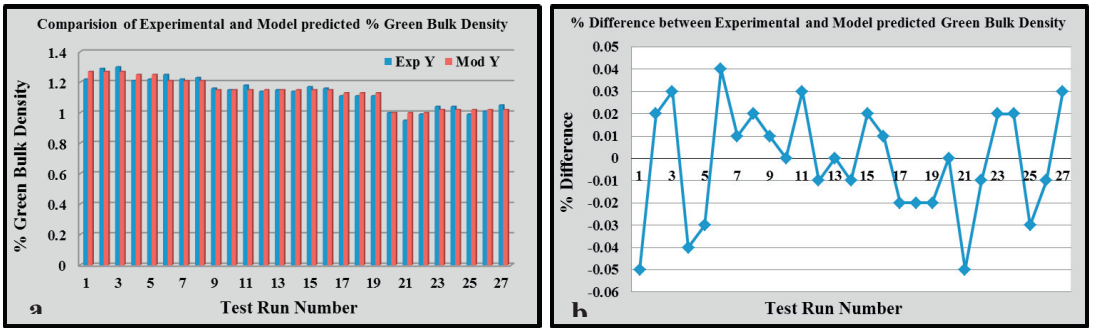

Fig. 3. (a) Comparison of Experimental and Model predicted % Green Bulk Density, (b) Percentage Deviation of Experimental and Model predicted Green Bulk Density.

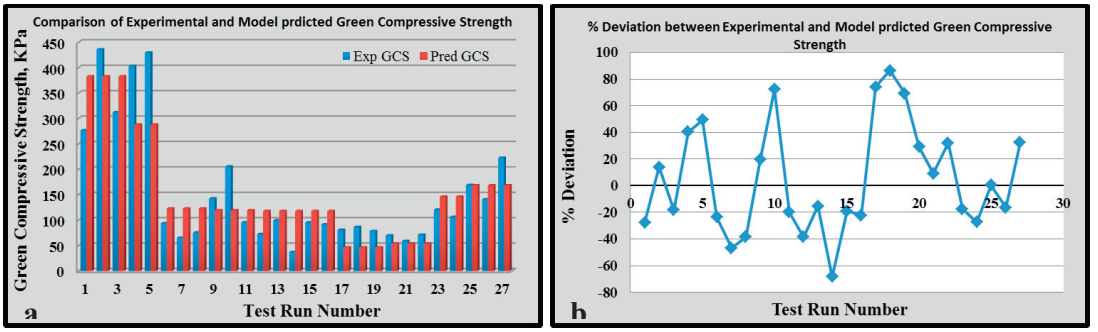

Fig. 4. (a) Comparison of Experimental and Model predicted Green Compressive Strength, (b) Percentage Deviation of Experimental and Model predicted Green Compressive Strength.

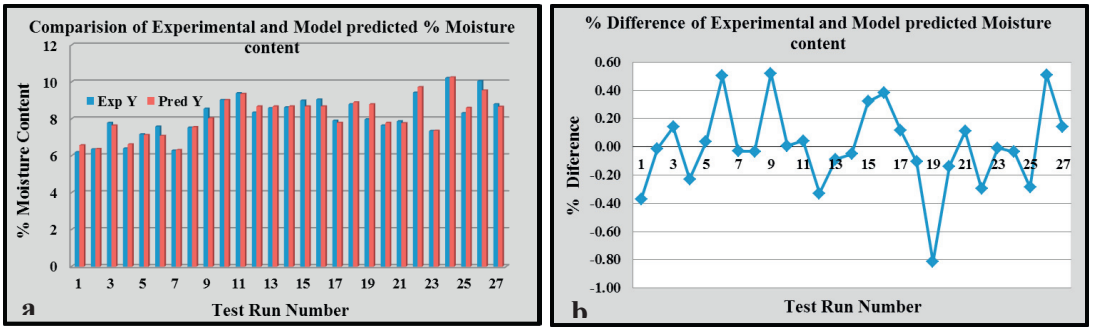

Fig. 5. (a) Comparison of Experimental and Model predicted % Moisture Content, (b) Percentage Deviation of Experimental and Model predicted Moisture Content.

The experimentally measured and model predicted green compressive strength is shown in Fig. 4, the strength of the mould was found to decrease while the porosity increased linearly with an increase in water; the water and air permeability increased and the apparent density decreased **[8]**. When the water is added to the β-hemihydrate the hydration process begins and the nuclei of the gypsum crystals start to absorb the neighbouring particles and the gypsum crystals start to grow in short length and interlock each other and form bonding around the silica sand particles. Water molecules act as carriers for the ions to move and to form a crystal structure, there is a saturation limit where the gypsum particles can't absorb more water, and the excess water stays back over the link and increases the plasticity, thus weakening the structure. This excess water can be driven off by drying the mould at room temperature or oven, when the drying (baked) temperature increases above 150°C the free water is removed and the β-hemihydrate is formed back thus giving strength to the mould. With further increase in temperature above 300°C chemically bonded water is also driven off and Anhydrite III is formed **[1]**. If the baked temperature is not optimized the moisture would be present in the mould. Fig. 5 shows the moisture content present in the mould even after baking, which leads to the porous structure and a collapse of the mould when the molten metal enters. The leftover moisture increases linearly with increase in percentage of hemihydrate and water **[16]**.

4. Conclusions

The amount of water requirement differs significantly based on the type of hemihydrate used in slip casting process; α-hemihydrate consumes less water than the β-hemihydrate plaster. The α-hemihydrate develops needle type crystal structure which interlocks firmly during rehydration resulting in improved strength of the mould. Whereas β-hemihydrate develops short entangles crystals in the structure. Hydration of the hemihydrates in the 3DP system is different from the slip casting process as water is pre-mixed with plaster and the liquid binder is sprayed on the powder bed. The premixed moisture makes the particles ready for the nucleation process and as soon as the binder strikes the top surface of the powder, the hydration process begins forming the bonds. When the water percentage is increases the porosity increases and the density of the mould decreases. At the same time, permeability should be optimized to allow the hot gases to escape from the molten metal. It was conclude that less (33%) percentage of plaster and moisture (2%) produce better strength in spite of the dimensional changes. Whereas the higher plaster content (53%) with 2% water results in minimum or nil volume change but the strength of the mould is reduced. However, by adding suitable additives both dimensional change and the strength of the moulds can be modified to meet the specific application of the casting.

Reference:

[1] Gergely Sirokman., "Synthesis, Dehydration, and Rehydration of Calcium Sulfate (Gypsum, Plaster of Paris)", Journal of Chemical Education., 2014, 91, 557-559
[2] Elisabeth Badens., Stephane Veesler., Roland Boistelle., Crystallization of gypsum from hemihydrate in presence of additives", Journal of Crystal Growth, 198/199, 1999, 704-709
[3] U. Ludwig, N. B. Singh, Cement Concrete Res. 8 (1978) 291-300.
[4] A. J. Lewry, J. Williamson, J. Mater. Sci. 29 (1994) 5279-5284.
[5] P. Coquard, R. Boistelle, Int. J. Rock Mech. Min. Sci. and Geomech. Abstr.31 (1994) 517
[6] Y. Kato, M. Matsui, K. Umeys, Gypsum Lime 166 (1980) 83
[7] L. Amathieu, R. Boistelle, J.Crystal Growth 79 (1986) 169
[8] N.B.Singh, B. Middendorf, Prog. Crystal Growth Character. Mater. 53 (2007) 57-77
[9] Kyung-Min Song, Jonathan Mitchell, Lynn F. Gladden, "Observing Microstructural Evolution During Plaster Hydration "Diffusion Fundamentals, 10 (2009) 22.1 - 22.3
[10] Q. L. Yu and H.J.H. Brouwers, Microstructure and mechanical properties of β-hemihydrate produced gypsum : An insight from its hydration process. Construction and Building Materials 25(2011) 3149-3159
[11] S. Z. Mohd. Nor, R. Ismail and M. I. N. Isa, "Terengganu's Silica Sand as moulding material for

Investment – cast copper alloys", UMT 11th International Annual Symposium on Sustainability Science and Management, Malaysia, 2012, 1306-1310

[12] W.K. Luk and B.W. Darvell, Effect of burnout temperature on strength of gypsum bonded investments, Dentals Materials 19 (2003) 552-557.
[13] A. C. J de Korte and H. J. H. Brouwers, "Hydration Modeling of Calcium Sulphates", ICCBT 2008, A, 39, 433-444
[14] Sohnel, O. and J. Garside, "Precipitation, Basic principles and industrial applications", First ed., 1992, Oxford: Butterworth-Heinemann Ltd.
[15] James F Bredt., Timothy C. Anderson., and David B. Russell., "Three Dimensional Printing Material system and Method", United States patent, US 7087109 B2., Aug. 26, 2003
[16] S. S. Bobby, "A preliminary Investigation of Gypsum bonded moulds by Three Dimensional Printing", International Journal of Research in Engineering and Technology, 2014, Vol 03, 06, 501-507.
[17] Frondel C, Dana's System of Minerolgy, 7th Edition, 1962.